



A CFD simulation of a single phase hydrocyclone flow field

by M.F. Dlamini*, M.S. Powell†, and C.J. Meyer*

Synopsis

The hydrodynamics of a hydrocyclone present a complex internal flow structure, the numerical simulation of which remains a non-trivial task. We report on three-dimensional water-only computational fluid dynamics (CFD) hydrocyclone flow field predictions and highlight some of the issues concerned with the development of a CFD model incorporating an air core. The potential for the application of CFD as a hydrocyclone design tool is also discussed. Physically realistic velocity profile predictions were obtained, which challenge the classical account of the hydrocyclone radial particle classification mechanism. A pressure field distribution consistent with literature reports was also predicted.

Keywords: hydrocyclone, computational fluid dynamics (CFD), classification mechanism

Background

Current hydrocyclone models, some of which are partially based on a qualitative understanding of the associated flow physics, are largely empirical. The bulk of these models can, in fact, be represented by simple partition curves that reflect the probability that governs whether a particle will report to either the overflow or underflow. Unfortunately, the application of these models is often restricted to the range of operating conditions and hydrocyclone geometries for which they were derived. This handicap thus restricts their scope of application and prohibits the possible extension to novel devices. Consequently, the need for continued complementary research via computational techniques such as CFD, which facilitates parametric investigations to be conducted, is established.

A correct understanding of the hydrocyclone flow and pressure fields is required if the particle classification that is effected within the device is to be modelled in a mechanistically meaningful and appropriate manner. Accounts of successful CFD hydrocyclone flow modelling are reported in the literature^{3,9,15} but insufficient detail is given on the procedural methodology adopted in setting up the CFD models. As such, no reproducible benchmark problems that can be used for CFD

model validation are available to other CFD practitioners. Consequently, we propose to establish and publish standard procedures for setting up a multiphase CFD hydrocyclone model. We intend to acquire the relevant knowledge and expertise by building up the CFD hydrocyclone model incrementally, in the order: single phase (water-only), multiphase (water/air) and multiphase (water/air/solids) flow, respectively. At present, we report on water-only hydrocyclone flow field simulations as well as the progress made in modelling multiphase flow.

Introduction

The applications of a hydrocyclone are based on its ability to separate particle suspensions in accordance with particle size, density and shape. The extreme versatility it exhibits in its applications is indicated by its capability for use as a thickener, a classifier or a concentrator, and a clarifier¹. Its mechanical simplicity deceptively suggests non-intricate and well-understood device hydrodynamics. On the contrary, complex flow features such as an intrinsically unstable air core and combined laminar and turbulent flow regimes are established. Furthermore, at practical operating conditions, rheologically complex slurries are treated that typically exhibit non-Newtonian behaviour, hence the added difficulty in the formulation of a mathematically sound definition of the internal flow physics. Consequently, improved understanding of the hydrodynamics of a hydrocyclone is still being sought in order that its full classification potential may be realized.

The hydrocyclone internal flow structure

The hydrocyclone flow structure may be classified into primary and secondary flow

* Department of Mechanical Engineering, UCT.

† Department of Chemical Engineering, UCT, Rondebosch, Cape Town, South Africa, mpowell@chemeng.uct.ac.za.

© The South African Institute of Mining and Metallurgy, 2005. SA ISSN 0038-223X/3.00 + 0.00. Paper received Jan. 2005; revised paper received Sep. 2005.

A CFD simulation of a single phase hydrocyclone flow field

patterns. The primary flow consists of two vertically opposed helical spiral fluid streams, which transport the distinct discharge products. Two secondary flow patterns that include the short-circuit and eddy flows are also formed, which contribute to inefficient hydrocyclone particle classification. In practical applications, the bulk flow structure is typically complemented by a centrally positioned air core.

The primary flow pattern

With reference to Figure 1, the pressurized fluid or slurry is fed tangentially through the inlet duct into the cylindrical chamber, where a strong swirl motion is established⁶, such as to yield the two vertically opposed spirals. The centrifugal forces arising from this motion cause solid particles to migrate to and concentrate at the cyclone wall^{4,6}. The coarse and denser particles are preferentially conveyed by the outer spiral and discharge as a thickened suspension⁴ at the cone's apex, to form the underflow. A second stream comprising finer particles of lower settling velocities discharges with the inner spiral through the vortex finder, located at the top of the hydrocyclone, to form the overflow. In this manner, the coarse and fine size fractions are separated. Depending on the circuit configuration and the final product requirements, the underflow may be recirculated for additional grinding while the overflow is processed in subsequent downstream processes.

Secondary flow features

The secondary short-circuit and eddy flow patterns are depicted in Figure 2. The short-circuit flow is confined to the region near the roof of the hydrocyclone and the wall of the vortex finder. Photographic evidence and visual inspection indicate that, for a slurry, the short-circuit flow path constitutes a concentrated band of coarse solid particles that by-pass classification and discharge with the overflow⁴. The vortex finder, in addition to discharging the overflow, is intended to minimize the short circuit flow¹. The eddy flow, on the other hand, is the direct result of the vortex finder discharge orifice failing to accommodate the entire overflow stream¹, such that it recirculates and joins the inlet stream.

Hydrocyclones experience very high liquid velocities in the vicinity of the central vertical axis that cause a pressure reduction capable of yielding a gas-liquid interface in the region of the core⁵. If operating conditions are such that either of the discharge orifices of the hydrocyclone is exposed to the atmosphere, the core region is transformed into a central air core⁵⁻⁶. It is commonly deduced that pressure differences instigate and maintain the air core. On the contrary, a new understanding of the mechanism leading to air core development due to Cullivan *et. al.*⁷ has evolved. Their CFD simulations, for which experimental validation was acquired, demonstrated air core development to be transport-driven as opposed to being pressure-driven.

The geometry assumed by an air core is operating condition dependent and may be in the form of a linear or wavy cylinder, extending in part or throughout the hydrocyclone length^{4,6}. The common understanding that the presence of an air core within a hydrocyclone is a desirable feature, because of implied vortex stability, is widely professed in the literature^{1,6}. The air core is also associated with the type of underflow discharge. The spray-type discharge indicates the existence of an air core⁸ and marks

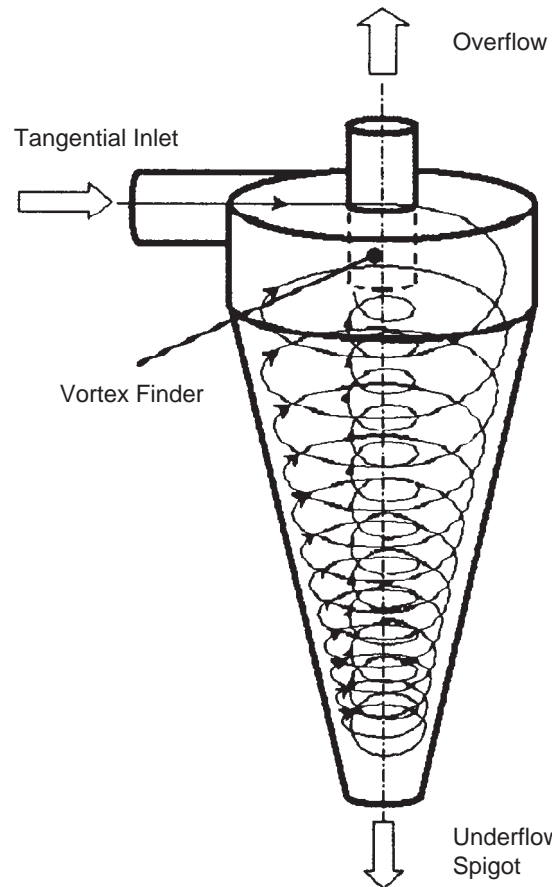


Figure 1—A hydrocyclone flow schematic

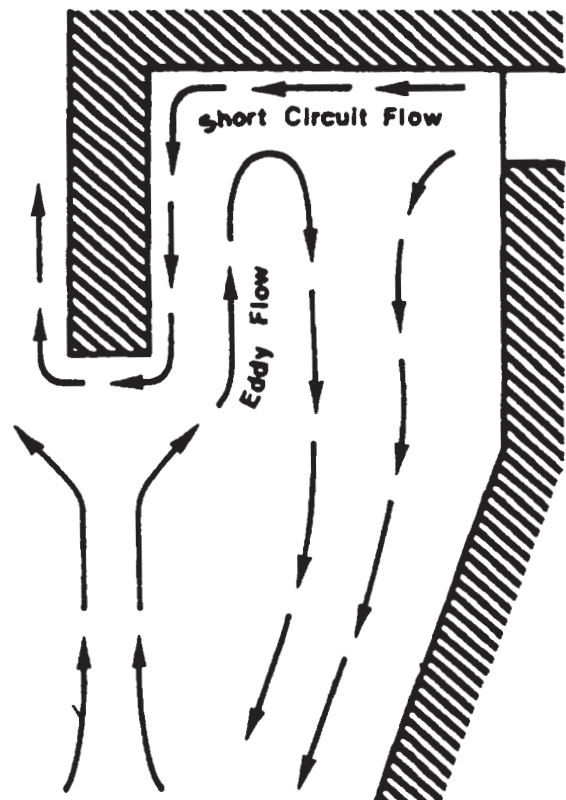


Figure 2—Hydrocyclone secondary flow features

A CFD simulation of a single phase hydrocyclone flow field

the condition where solids and liquid discharge in a spray, in the shape of a hollow cone, and with maximum removal of solids. The lack of an air core is indicated by the rope-type discharge⁸ in which the discharge is a rotating solid spiral.

The fluid velocity distribution

Any three-dimensional velocity within a hydrocyclone flow field may be resolved into three mutually perpendicular components, viz. the axial, radial and tangential velocity components. Pioneering work on fluid velocity component measurements was conducted by Kelsall⁴, via an optical study of a dilute suspension of aluminium particles. Kelsall⁴ measured the fluid tangential and axial velocity components at different horizontal levels along the length of the hydrocyclone and calculated the radial velocity component from continuity.

Axial velocity

The liquid axial velocity component is an indication of the magnitude of the two spirals depicted in Figure 1 and therefore determines the volumetric distribution of the product between the overflow and underflow streams¹. A locus or envelope of zero axial velocity is a significant feature of this velocity component and divides the outer downward flowing and the inner upward flowing fluid layers¹. The axial velocities increase with distance from the envelope, with the inner spiral having a considerably higher maximum velocity.

Radial velocity

Of the three velocity components, the radial component is the least in magnitude¹. Its magnitude increases radially outwards and reaches a maximum in the vicinity of the hydrocyclone wall. It is normally directed radially inwards, with the exception of eddy flow just outside the vortex finder¹. As a result, particles require a centrifugal force in order to settle against it, such as to be discharged as underflow. In a radial sense, particle classification is understood to result primarily from a centrifugal-drag force balance, with radial transport of small particles towards the core, throughout the conical section, and centrifugal drift of large particles towards the cyclone wall⁷. The faster settling coarser particles migrate to the cyclone wall, where the absolute fluid velocity is lowest, and discharge with the underflow. Conversely, the slower settling finer particles migrate radially inwards and are discharged with the overflow.

Tangential velocity

The tangential velocity increases traversing towards the core of the hydrocyclone, before decreasing rapidly at the interface with the air core. The associated velocity gradients are steepest in the region below the vortex finder. The tangential velocity profiles assume a compound vortex structure, known as a Rankine vortex, which constitutes free and forced vortices near the hydrocyclone wall and the central vertical axis, respectively. A parabolic peak, intermediate between the two vortex regions, marks a gradual transition between the two distinct and uniquely defined vortex structures.

The hydrocyclone pressure field distribution

The total pressure at any point in a hydrocyclone is the sum of the static and velocity pressure at that point¹⁰. Numerous factors reportedly contribute to pressure drop across a

hydrocyclone but the most noteworthy, which also consumes energy during its formation¹⁰, is the Rankine vortex. Of interest is the pressure drop that supposedly leads to the formation of a central air core. The pressure drop across the inlet and discharge ducts is also significant, due to its tendency to impose high energy expenditure pumping requirements. Unfortunately, despite the much needed knowledge of the pressure variation across the cyclone, of all the numerous empirical, semi-empirical and theoretical cyclone pressure drop relationships that have evolved, none proves to be universally applicable¹⁰.

CFD model description

This section, in accordance with our primary objective, outlines the procedural methodology adopted in setting up the CFD hydrocyclone model. The hydrocyclone flow field was modelled via the commercial CFD code Fluent v6. The tangential rectangular inlet number 1 hydrocyclone from the Monredon *et. al.*¹³ study, whose dimensions are listed in Table I, was used for the CFD model geometry. The symbols *d* and *h* represent component diameters and heights or lengths respectively. A three-dimensional structured butterfly-type mesh consisting of approximately 257 000 mesh volumes and a conformal inlet duct mesh was implemented. The use of a structured mesh enabled the application of the pressure-staggered option (PRESTO), via which the computational expense is considerably reduced, on account of the pressure field being stored on a mesh staggered from that of the velocities such that interpolation is not required for reconstruction of the pressure field during iterations¹⁴.

Boundary condition specification

An inlet velocity boundary condition type and a velocity of 2.28 m/s were specified at the duct inlet. Pressure outlet boundary condition types were specified at both hydrocyclone discharge orifices, at which a standard atmospheric pressure condition was prescribed. The radial pressure gradient that is established due to the swirl generated by the hydrocyclone flow field^{3,14} was accounted for by allowing for radial pressure distribution across the hydrocyclone discharge orifices. If a constant pressure is specified at the discharge orifices, the swirl is artificially suppressed and the internal hydrocyclone flow structure adversely influenced³. As per standard CFD practice, a no-slip wall boundary condition was specified at all hydrocyclone wall boundaries. Standard wall functions were used to approximate flow variables in the near-wall region.

Table I

CFD hydrocyclone model dimensions

Component	d (mm)	h (mm)
Main chamber	75	75
Inlet duct	25	75
Vortex finder	25	50
Spigot	12.5	25
Conical chamber (20° cone angle)	75	186

A CFD simulation of a single phase hydrocyclone flow field

Mathematical model description

The Reynolds Stress Model (RSM), which has been shown^{3,9} to represent the minimum order of accuracy for modelling hydrocyclone flow turbulence, was implemented to provide turbulence closure. The Reynolds stresses were modelled via Equation [1], where the terms represent: (I) the rate of change of Reynolds stresses, (II) stress generation, (III) energy dissipation, (IV) pressure strain effects and (V) the diffusion of Reynolds stresses. The adopted terminology is consistent with the literature^{11,14}.

$$\frac{Du'_i u'_i}{Dt} = - \left[\underbrace{u'_j u'_k \frac{\partial \bar{u}_i}{\partial x_k}}_{(I)} + \underbrace{u'_i u'_k \frac{\partial \bar{u}_j}{\partial x_k}}_{(II)} \right] - 2\nu \frac{\partial u'_i \partial u'_j}{\partial x_k \partial x_k} + \frac{p'}{\rho} \left(\frac{\partial u'_i}{\partial x_j} + \frac{\partial u'_j}{\partial x_i} \right) - \frac{\partial}{\partial x_k} \left[\underbrace{u'_i u'_j u'_k}_{(V)} - \nu \frac{\partial u'_i u'_j}{\partial x_k} + \frac{p'}{\rho} (\partial_{jk} u'_i + \partial_{ik} u'_j) \right] \quad (I) \quad (II) \quad (III) \quad (IV)$$

Careful consideration should be given to modelling the pressure strain term, i.e. term IV¹⁴. The modelling considerations are particularly significant with high swirl flows for which the correlation between the fluctuating pressure and velocity is sensitive¹⁴. CFD studies due to Cullivan *et. al.*¹⁴ identified the quadratic pressure strain model as a lower bound for turbulence modelling of hydrocyclone flow¹⁴. In accordance with the simulation strategy adopted by Brennan⁹, it was intended to use a water-only solution flow field as input for the multiphase flow simulation. Consequently, the linear pressure strain model was employed in this work in order to maintain solution stability because the more sensitized quadratic pressure strain model was found to aggravate solution instability with the multiphase flow field, for the specified grid density. Velocity and turbulence quantities were discretised via the QUICK scheme while the PRESTO and SIMPLEC schemes were employed for pressure discretization and pressure-velocity coupling, respectively.

Although it is suggested by some authors^{12,15} that the solution flow field is initiated via a steady state solver, insufficient detail is given on the appropriate input parameters necessary to obtain a converged solution. Attempts to initiate the simulation at inlet velocities less than the operating value of 2.28 m/s, as suggested by Schuetz *et. al.*¹², gave diverged solutions. Solution convergence via a steady state solver was thus achieved through the application of under-relaxation factors of 0.35 and 0.5 to the momentum and turbulent viscosity equations, respectively. A cycling in the residuals, indicating the inadequacy of the steady state solver in resolving the transient hydrocyclone flow field, as reported by Slack *et. al.*³, was observed. The flow was subsequently simulated transiently, with convergence criteria of 0.001 specified for all solution variables. A total flow time in excess of two mean residence times was simulated and solution convergence achieved at each time step. The significance of the total simulation period is that it permits meaningful predictions to be derived because it is greater than the maximum particle retention period, which was assumed to be equivalent to the total time taken by a particle to travel from the inlet to the spigot and back up such as to be discharged with the overflow stream. In accordance with reports due to Slack *et. al.*³, adoption of the transient solver

significantly improved the definition of the velocity and pressure field profiles.

Results

Predicted velocity profiles

The predicted liquid velocity component trends were consistent with those due to Kelsall⁴. With respect to Figure 3, the component velocity profile data acquisition loci were lines of intersection of the x-y plane and horizontal planes lying at various depths below the roof of the cyclone. Typical velocity profile predictions sampled at a 120-mm depth are depicted in Figures 4, 6 and 7.

The positive core and surrounding negative axial flow field depicted in Figure 4 give evidence of the existence of a locus or envelope of zero axial velocity, within which fluid motion is directed upwards and downwards beyond its periphery. This observation serves to confirm the establishment of the vertically opposed overflow and underflow discharge streams. An increase in the absolute values of the axial velocity component was predicted with increase in distance from the envelope of zero axial velocity. The exhibited increase was greater in the upward than the downward direction of flow.

Figure 5 depicts the locus of zero axial velocity. In accordance with reports due to Leith¹⁰, the horizontal axis intercept of the locus of zero axial velocity was predicted to migrate radially inwards, traversing down the length of the cyclone. The insignificant deviations from this trend, as depicted in Figure 5, may be attributed to the inability by the vortex finder discharge orifice to adequately accommodate the overflow stream. This results in instantaneous retardation and build-up of upward core flow, which in turn causes radial displacement of the interface between upward and downward-directed flow or the locus of zero axial velocity. Recirculating streams, as evidenced by the eddy flow set-up in the vicinity of the tip of the vortex finder, are also established. The larger radial displacement of the locus of zero axial velocity in the immediate vicinity of the tip of the vortex finder, is indicative of short-circuit flow.

Of the three liquid velocity components, the radial component represented the least in magnitude. Contrary to the classical understanding, the CFD predictions revealed that the radial velocity component is not always directed radially

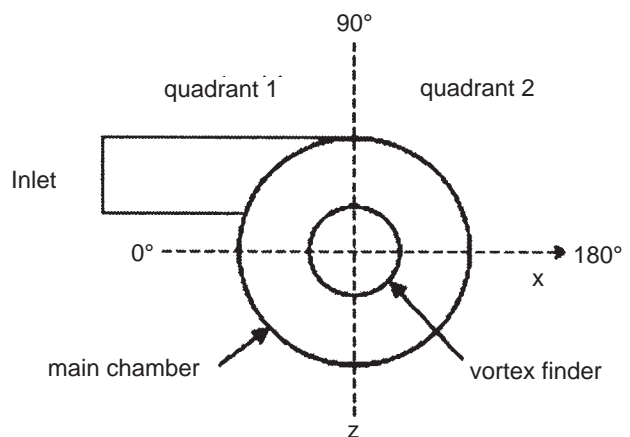


Figure 3—CFD hydrocyclone model coordinate system descriptor

A CFD simulation of a single phase hydrocyclone flow field

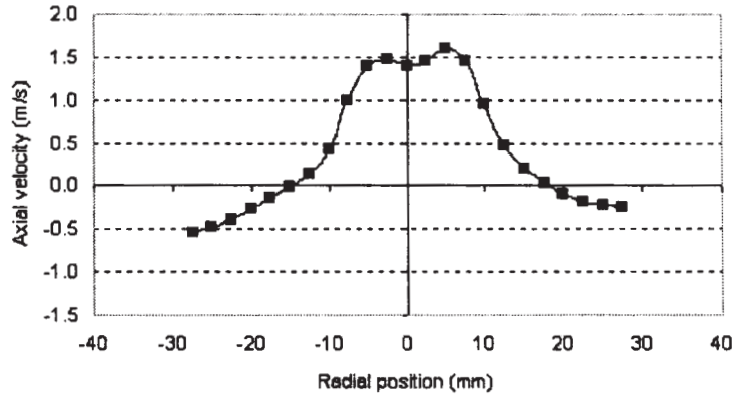


Figure 4—Predicted liquid axial velocity profile (120 mm)

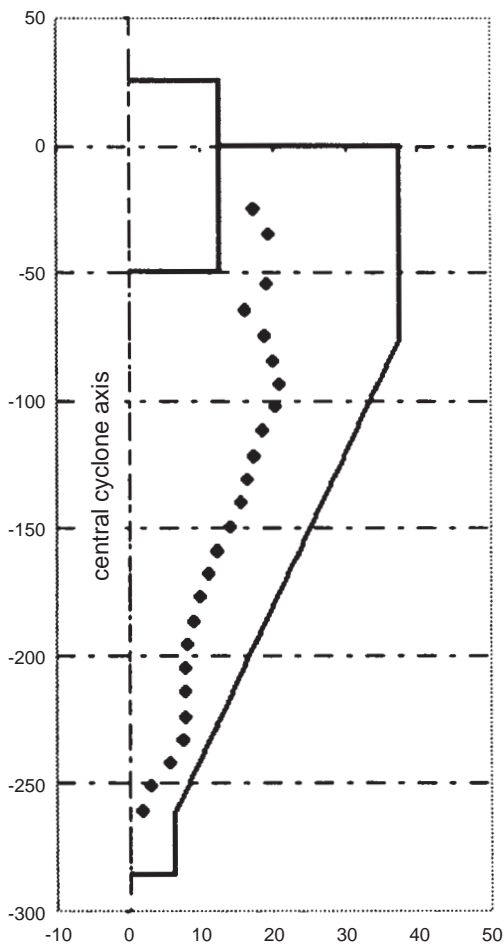


Figure 5—Locus of zero axial velocity

inwards. As depicted in Figure 6, the indication is that within a significant portion of the positive x -axis direction, the radial velocity field is, for the inlet flow direction depicted in Figure 3, directed radially outwards. A similar observation was made by Cullivan *et. al.*¹⁴ who noted an asymmetric alternating radial particle-transport direction across the length of the hydrocyclone. As such, provided the fluid and solid particle motion is approximately homogeneous such that fluid drag may be neglected, the centrifugal force is supplemented and the centrifugal drift of particles further enhanced. As a result, and on account of the relatively minute numerical values exhibited by the radial velocity field,

the indication is that radial particle displacement and classification are predominantly due to the centrifugal force and that radial particle migration is primarily a mass diffusion effect. The relatively insignificant negative flow field established in the positive x -axis direction of Figure 6, which is indicative of radially inward-directed flow, may be attributed to bulk flow wall reflection effects.

The RSM accurately predicted the tangential velocity-associated Rankine vortex structure depicted in Figure 7. The Rankine vortex, by effecting solid body rotation at the core of the flow field, via forced vortex motion, induced a negative core pressure.

Predicted pressure profile

The development of the flow pressure field was marked by the initial establishment of sub-atmospheric pressures within the spigot and vortex finder. During this phase, the remainder of the body of the hydrocyclone constituted an asymmetric positive pressure field, which exhibited a positive gradient, traversing radially outwards. Atmospheric exposure of the discharge orifices led to the formation of a negative core pressure, with high pressure gradients being predicted in the vicinity of the central axis. Figure 8 depicts the predicted pressure field, in which the values indicated on the pressure scale are relative to an atmospheric pressure value of 101 325 pascals.

Geometry effects

Inlet geometry effects on the hydrocyclone flow field were investigated by examining the turbulence intensity of the flow fields in the feed entry section of circular (25 mm diameter) and rectangular (20 mm x 25 mm) cross-sectional inlet hydrocyclones, with the overall dimensions given in Table I. In accordance with reports due to Kelsall¹⁶, excessive turbulence prevails within the feed entry section of a hydrocyclone, where the inlet stream comes into contact with the swirling flow field contained within the main chamber. The turbulence mixing subsequently effected is reportedly due to the resultant shock effects. The turbulent kinetic energy per unit mass, k , which is a measure of the energy generated via the fluctuating turbulent velocity components of a turbulent flow field, was used to quantify and contrast the turbulence intensity levels. With respect to Figure 3, k was determined in quadrants 1 and 2, at a depth of 12.5 mm below the roof of the hydrocyclone and at a radial position midway between the vortex finder and main chamber walls.

A CFD simulation of a single phase hydrocyclone flow field

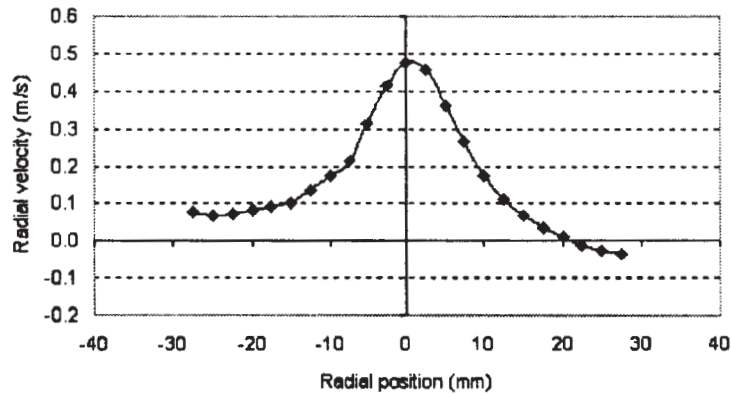


Figure 6—Predicted liquid radial velocity profile (120 mm)

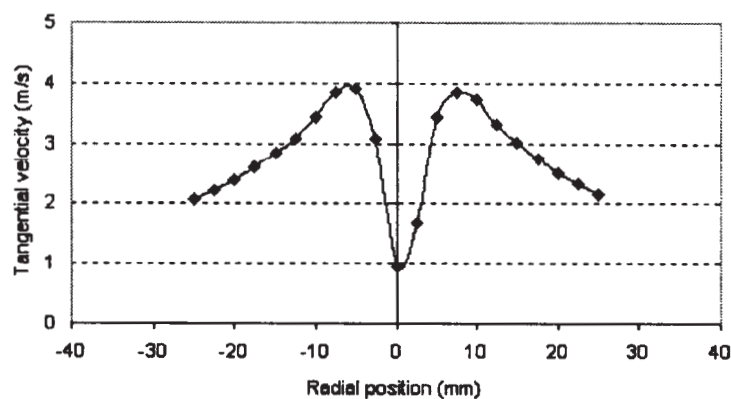


Figure 7—Predicted liquid tangential velocity profile (120 mm)

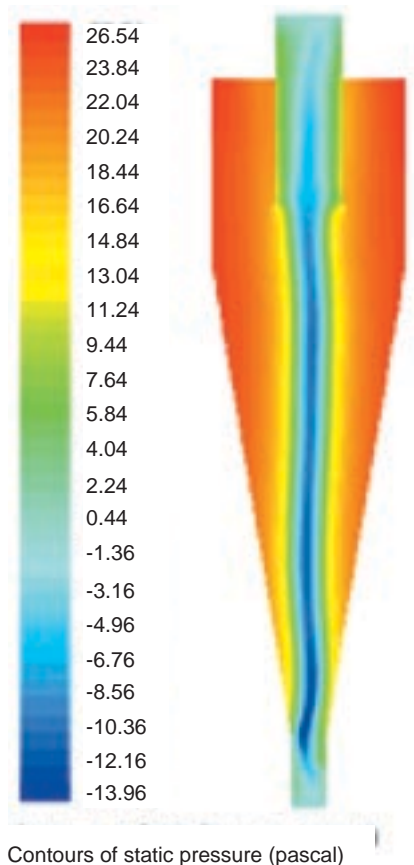


Figure 8—Hydrocyclone steady state pressure field

Equispaced data acquisition positions spanning an angular displacement of 180° were used, with the negative x-coordinate direction representing the datum.

The variation of k with angular displacement is depicted in Figure 9. The rapid increase in k with increase in angular displacement, up to a maximum at 90°, for the circular cross-sectional inlet hydrocyclone configuration, serves to confirm the high intensity of turbulence within the feed entry section. Subsequently, the incoming fluid stream is progressively decelerated, hence a progressive reduction in the momentum imparted onto the stagnant fluid stream, which, in turn, effects a decrease in k . Finally, on account of the swirl motion of the bulk flow, the flow field assumes a near-constant angular velocity and exhibits minimal turbulent velocity fluctuations, hence k remains approximately constant.

The flow field arising from the hydrocyclone with a rectangular cross-sectional inlet results in an average k -value of approximately 0.1. Its relatively less steeper inlet zone k -gradients are indicative of the establishment of near-equilibrium inlet-swirl flow conditions. Such steady flow conditions favour the operation of a hydrocyclone, since feed behaviour instability hampers its performance¹. The different inlet duct-main chamber interface geometries account for the variation in the shock effects exhibited within the feed entry sections of the variable cyclone geometric configurations. The numerical predictions demonstrate the potential for CFD to be used as a design tool to facilitate hydrocyclone concept design evaluation and optimization, prior to prototyping. The

A CFD simulation of a single phase hydrocyclone flow field

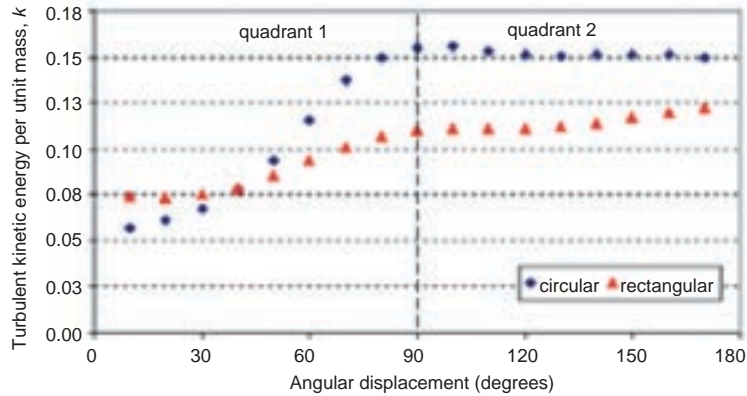


Figure 9—Variation of turbulent kinetic energy per unit mass in hydrocyclone feed entry section

analysis of turbulence, along with a study of the influence of inlet geometry on turbulent back-mixing, are key areas that will form the continuation of this work.

Preliminary multiphase flow investigations

Preliminary investigations aimed at establishing a suitable procedural methodology for modelling multiphase (water/air) hydrocyclone flow fields were undertaken. It was attempted to artificially develop an air core by introducing air as part of the feed stream of a fully developed water-only flow field with a negative core pressure. In accordance with the simulation strategy adopted by Brennan⁹, the sole recirculation of air across the overflow and underflow discharge boundaries was effected by setting the backflow volume fraction of air to unity, such as to artificially develop the air core from both discharge orifices. In a similar fashion to the actual physical process, the numerical solution exhibited extreme instability, coupled with divergent behaviour, during the air core inception phase. The Algebraic Slip Mixture Model was employed in modelling the multiphase flow field, for which air core inception was successfully simulated. The results indicated that a negative core pressure supports air core inception and the central location thereof, while the subsequent development of the air column is a dual function of pressure-driven gaseous diffusion and convective transport. We acknowledge that the presence of a stable air core is instrumental in ensuring effective hydrocyclone classification, particularly for minerals processing applications. It thus remains to develop a procedure that may be consistently implemented to obtain a fully developed air core with the CFD hydrocyclone models.

Concluding remarks

The turbulence and auxiliary models suited to the CFD modelling of single phase and multiphase hydrocyclone flow fields, via specific discretization schemes, were identified. Numerical predictions were obtained, which reflect physically realistic hydrocyclone velocity and pressure field profiles. The procedural methodology for development of the air core was explored and numerical predictions providing insight into the probable mechanism for inception and development thereof, have been obtained. The numerical investigation, which enabled the quantification of the effects of different inlet geometries on the internal flow field, demonstrated a potential useful application of CFD in hydrocyclone parametric geometry optimization. Numerical studies of multiphase flow fields are a subject of future research.

Acknowledgements

The authors wish to acknowledge the assistance of Dr M. Slack of Fluent Europe Ltd. and Dr M. Brennan of the University of Queensland, Australia.

References

1. KELLY, E.G. and SPOTTISWOOD, D.J. *Introduction to Mineral Processing*. New York: John Wiley and Sons, Inc., 1982.
2. SLACK, M.D. AC-cyclone separator, Fluent Europe Ltd., 2002.
3. SLACK, M., DEL PORTE, S., and ENGELMAN, M.S. Designing automated computational fluid dynamics tools for hydrocyclone design, in *Proceedings Hydrocyclones '03*, Cape Town, South Africa, 24–26 September, 2003.
4. KELSALL, D.F. A study of the motion of solid particles in a hydraulic cyclone, *Transactions Institute Chemical Engineers*, vol. 30, 1952. pp. 87–104.
5. DYAKOWSKI, T. and WILLIAMS, R.A. Modelling turbulence flow within a small diameter hydrocyclone, *Chemical Engineering Science*, vol. 48, no. 6, 1993. pp. 1143–1152.
6. CHAKRABORTI, N. and MILLER, J.D. Fluid flow in hydrocyclones: a critical review, *Mineral Processing and Extractive Metallurgy Review*, vol. 11, 1992. pp. 211–244.
7. CULLIVAN, J.C., WILLIAMS, R.A., and CROSS, C.R. Understanding the hydrocyclone separator through computational fluid dynamics, Institution of Chemical Engineers, *Transactions IChem*, vol. 81, Part A, 2003. pp. 455–466.
8. WILLIAMS, R.A. *et al.* Using electrical impedance tomography for controlling hydrocyclone underflow discharge, *Control Engineering Practice*, vol. 5, no. 2, 1997. pp. 253–256.
9. BRENNAN, M.S. Multiphase CFD simulations of dense medium and classifying hydrocyclones, *Proceedings of the Third International Conference on CFD in the Minerals and Process Industries*, CSIRO, Melbourne, Australia, 10–12 December, 2003.
10. LEITH, D. Cyclones, *Handbook of Powder Science and Technology*, M. E. Fayed and L. Otten, (eds.). New York: Chapman and Hall, 1997. pp. 730–753.
11. WHITE, F.M. *Viscous Fluid Flow*, 2nd ed. Singapore: McGraw-Hill, Inc., 1991.
12. SCHUETZ, S., MAYER, G., BIERDEL, M., and PIESCHE, M. Investigations on the flow and separation behaviour of hydrocyclones using computational fluid dynamics, 29 April 2003, accepted for publication by *International Journal of Mineral Processing*.
13. MONREDON, T.C., HSIEH, K.T., and RAJAMANI, R.K. Fluid flow model of the hydrocyclone: an investigation of device dimensions, *International Journal of Mineral Processing*, vol. 35, 1992. pp. 65–83.
14. CULLIVAN, J.C., WILLIAMS, R.A., DYAKOWSKI, T., and CROSS, C.R. New understanding of a hydrocyclone flow field and separation mechanism from computational fluid dynamics, *Minerals Engineering*, vol. 17, 2004. pp. 651–660.
15. SLACK, M.D., PRASAD, R.O., BAKKER, A., and BOYSAN, F. Advances in cyclone modelling using unstructured grids, *Transactions Institute Chemical Engineers*, vol. 78, 2000. pp. 1098–1104.
16. KELSALL, D.F. A further study of the hydraulic cyclone, *Chemical Engineering Science*, vol. 2, 1953. pp. 254–272. □

SPOTLIGHT

INFACON XI

The International Committee of Ferroalloys (ICFA) awarded INFACON XI to India at its meeting during INFACON in Cape Town in February 2004. The INFACON Congress has been held in Southern Africa on three occasions since its inception in 1974 when Mintek, FAPA (The South African Ferro Alloy Producers Association) and The SAIMM founded this three yearly, mostly technical event. Mintek hosts the secretariat for ICFA and The SAIMM plays a major role in organising the Congress when it is held in South Africa. INFACON XI will also be the third time that the Congress is held in Asia, the first being in Tokyo, Japan and the second in Beijing, China. It is most appropriate that the INFACON XI, to be held in New Delhi from 18–21 February 2007, is being held in Asia again. The growth rates in Asia and in China and India, in particular, makes this an exciting time to be holding INFACON there. The rapid growth in carbon and stainless steels is generating increasing demand for ferroalloys in the region.

The local production of ferroalloys and imports from e.g. South Africa are increasing more rapidly than elsewhere. The Indian Ferro Alloy Producers Association (IFAPA) theme of 'Innovations in the Ferroalloy Industry' has been chosen to reflect the increasing challenges faced by the industry globally. Technical papers are being sought for INFACON XI that address the following topics: improved equipment design, novel raw material processing, pioneering operations management and productivity systems, advanced control and information technology, improved energy efficiency and reduced environmental impact. The categories cover the major ferroalloys ferrochromium, ferromanganese and ferrosilicon as well as the minor ones, including vanadium, molybdenum, niobium, and silicon.

IFAPA has recently issued the announcement and call for papers for INFACON XI. The information is being distributed to delegates who attended INFACON X and via the respective ICFA representatives. The contact with IFAPA is via Mr T.S. Sundaresan Secretary General at ifapa@vsnl.net or ifapa@hotmail.com. Mr Sundaresan is also the INFACON XI Congress secretary. IFAPA are busy establishing a web site. Mr P. Roy, Executive in charge Ferro Alloys & Minerals of Tata Steel, is the chairman of INFACON

XI and Mr R.K. Saraf, Vice-chairman and managing director of FACOR is the vice-chairman. Other members of the committee include Mr D. Ashok of Nava Bharat Ferro Alloys who attended the ICFA meeting in Cape Town as a representative of IFAPA.

Dr Barcza, chairman of ICFA, was invited to attend a meeting with IFAPA during the jointly arranged 2nd Indian Ferroalloys Conference in September in New Delhi that was organized together with *Metal Bulletin*. This event afforded the 500 delegates an excellent opportunity to appreciate the excellent facilities and capabilities of the hosts for INFACON XI. The meeting with IFAPA covered various items that could be of assistance to the committee in planning INFACON XI.

The items covered included the organising committee and sub-committee structures and, in particular, the importance of the technical programme and publication committees. An exhibition is also planned during INFACON XI.

The SAIMM provided IFAPA with a comprehensive file containing all relevant information about the planning and organizing of INFACON X. This type of interaction is of great value to the organizers of subsequent events. Key considerations included the updating of the delegates' list to distribute the announcement and call for papers, assistance with identifying referees for the technical papers and support from ICFA members and representatives other ferroalloy producers associations. It was agreed that greater participation from producers in the former Soviet Union and in countries such as Russia, Kazakhstan and the Ukraine would also be sought.

INFACON XI plans to attract close to 90 technical papers and plenary and keynote presentations and over 300 delegates from outside India. Local support is expected to raise the participation to over 500 delegates. The support of the global ferroalloy industry is being sought to make INFACON XI one of the most successful congresses held to date. The hard work of the INFACON XI organising committee will no doubt be rewarded accordingly and we wish them every success with this first INFACON in India. u